Pd–Ni hydrogen sponge for highly sensitive nanogap-based hydrogen sensors

Eunyeong Lee [a,1], Junmin Lee [a,1], Jin-Seo Noh [a], Wonkyung Kim [a], Taeyoon Lee [b], Sunglyul Maeng [c], Wooyoung Lee [a,*]

[a] Department of Materials Science and Engineering, Yonsei University, 262 Seongsanno, Seodaemun-gu, Seoul 120-749, Republic of Korea
[b] Nanobio Device Laboratory, School of Electrical and Electronic Engineering, Yonsei University, 262 Seongsanno, Seodaemun-gu, Seoul 120-749, Republic of Korea
[c] Department of Electronic and Electrical Engineering, Woosuk University, Wonju, Jeollabuk-do 565-701, Republic of Korea

ARTICLE INFO

ABSTRACT

We have successfully fabricated sub-100 nm nanogaps in Pd–Ni alloy thin films on an elastomeric substrate by simple stretching. The nanogaps-containing Pd–Ni films were utilized as hydrogen-sensing sponges and their performance was demonstrated to dominate over the performance of similar mobile thin films comprised of pure Pd in major aspects such as the response time, sensitivity in high H_2 concentrations, and H_2 detection limit. Notably, $Pd_{87.5}Ni_{12.5}$ hydrogen sensing sponges showed ultra-high sensitive and reversible On-Off behaviors and low detection limit of ∼100 ppm, which were attributed to the reduced nanogap width and the enhanced volume expandability of Pd–Ni lattice. The effects of Ni added to Pd and a search for an optimum Ni concentration were also systematically studied.

1. Introduction

Nanoscale gaps have achieved great attention in various areas including single-electron transistors [1], molecular switching devices [2], and chemical sensors [3] due to their unique structural features. Particularly, nanogaps used for chemical sensing have demonstrated unusual characteristics such as On-Off operation, high sensitivity, and fast response compared to the conventional sensors. Controlling the gap width is a critical requisite for enhancing the sensing properties further, thereby realizing optimal sensors. However, fine control of the nanogap width and large-scale fabrication of the nanogaps are still challenging.

Nanogaps in palladium (Pd) have been intensively investigated for hydrogen gas (H_2) sensors, which was demonstrated a decade ago using Pd mesowire arrays. Although break junctions in the Pd mesowire arrays allowed the sensors to operate in an ideal On-Off manner [4], they still suffered from some serious issues such as the complex nanogap formation process and poor H_2 detection limit. To tackle those issues, various types of nanogap-utilizing H_2 sensors were brought forth, including nanowire or nanotube arrays and ultra thin films [5–10]. However, all the methods faced more or less fundamental problems: (i) the indiscernibility of H_2 concentrations above 2% due to the α-phase to β-phase transition, (ii) the immobility of the substrate limiting the H_2-sensing dynamics,

and (iii) the difficulty of nanogap width control restricting H_2 detection limit. Recently, a noble nanogap-based sensing method using highly mobile thin films on an elastomeric substrate (MOTIFE), where cracks were formed in a Pd film on the PDMS substrate by tensile straining, was developed [11]. This novel lithography-free method relieved the difficulty in nanogap formation with and enhanced the H_2-sensing dynamics due to the substrate mobility. However, the Pd MOTIFE showed the relatively high H_2 detection limit that is most likely related to the wide gap width in Pd film.

In this work, we have developed a highly effective method to lower the H_2 detection limit of the nanogap-based hydrogen sponge sensors through alloying Pd with Ni. Adding Ni to Pd could provide two advantages for detecting low H_2 concentrations: reduction of the nanogap width and increase of the relative volume expansion of films on H_2 absorption. Although the Ni inclusion may also enhance the H_2 detection discernibility, it is true that the increase in Ni content can lead to a hydrogen solubility decrease in the H_2 sponge sensors. Therefore, we have made efforts to find an optimum Ni concentration in Pd as a trade-off between the increase of the hydrogen sensibility and the decrease of the hydrogen solubility.

2. Experimental methods

The elastomeric substrates were fabricated by mixing Polydimethylsiloxane (PDMS) monomer (Sylgard 184 Silicon Elastomer Base, Dow Corning) with the curing agent at the weight ratio of 10:1, followed by curing the mixture at 75 °C for 4 h [12]. The PDMS substrate thickness was 0.75 mm and its size was 20 mm × 10 mm. On the PDMS substrates, Pd—Ni thin films with the size of 10 mm × 10 mm were deposited by co-sputtering from Pd and Ni targets at room temperature. The base pressure was 2×10^{-6} Torr and the powers applied to the Pd and Ni targets were adjusted to vary the Ni to Pd composition. The film thickness was fixed at 10 nm. Ni content in the deposited alloy films was analyzed by an energy dispersive X-ray spectrometer (EDX), and it was controlled in the range from 0 to 20 at%. The alloy formation of the deposited films was confirmed by X-ray diffraction (XRD) analysis. Nanogaps were introduced in the deposited films by simply stretching the film/elastomeric substrate. The surface morphology of Pd—Ni films and the gaps was observed using scanning electron microscopy (SEM, JSM-6500F) and atomic force microscopy (AFM, VEECO).

To measure the electrical current change of a Pd—Ni film sensor, two electrical contacts were formed at the ends of the film, which were connected to a current source-measuring unit (Keithley 236). The test film was placed inside a sealed gas chamber with a volume of 250 mL. The H_2/N_2 gas mixture intermixed with a desired concentration ran through the chamber and the chamber was maintained at nearly atmospheric pressure and room temperature. The Pd—Ni MOTIFE sensors were tested over the range of 0—10% of hydrogen concentrations, and the real-time electrical resistance or current change caused by H_2 absorption and desorption was detected at room temperature.

3. Results and discussion

The nanogap fabrication process in a Pd—Ni film on PDMS substrate is schematically shown in Fig. 1. The first step is to deposit a Pd—Ni film with a desired composition on the PDMS substrate (Fig. 1(a)). Both Pd and Ni elements were distributed in the film, as shown from an EDX element map in Fig. 1(a). A tensile strain (25% in this case) is applied to elongate the Pd—Ni film/PDMS substrate. Under this tensile strain, the film cracks linearly perpendicular to the straining direction and buckles by the poisson ratio ($\upsilon = 0.5$) in the parallel direction (Fig. 1(b)). Upon removing the tensile strain, the elastomeric substrate easily recovers to the original position, and the stretched Pd—Ni film pieces overlap with neighboring pieces (Fig. 1(c)). The exposure to H_2 produces volume expansion of the broken films by the incorporation of H atoms, and the subsequent removal of H_2 causes the films to shrink back to the equilibrium dimensions (Fig. 1(d))[11], which generates perfect nanogaps in the Pd—Ni films.

The nanogap width was analyzed by AFM. Fig. 2(a) shows a gap in a pure Pd film on PDMS substrate for comparison, which was prepared by the same method. The gap width is 380 nm on top and the average width of the gradually narrowing gap is estimated to be 218 nm. In contrast, the gap in a $Pd_{87.5}Ni_{12.5}$ film exhibits an average width of 61.8 nm, about
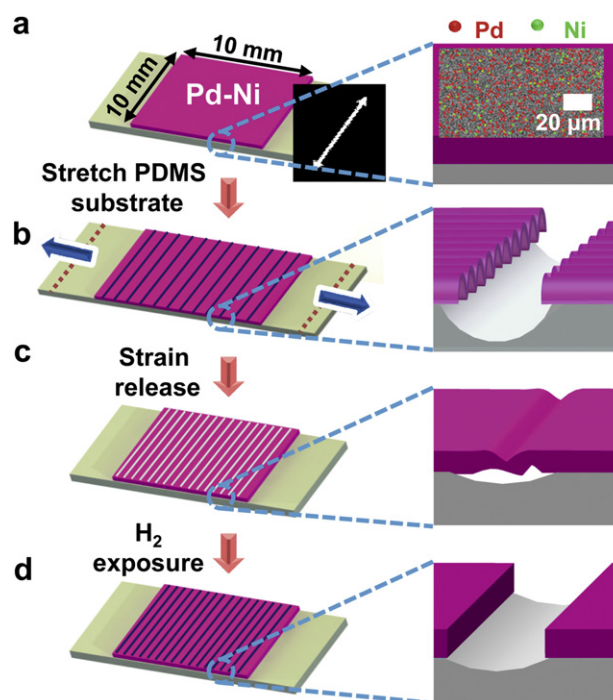

Fig. 1 — Schematic of the fabrication process of nanogaps in a Pd—Ni thin film on a PDMS substrate by mechanical stretching: (a) Step 1, deposition of a PdNi thin film on a PDMS substrate using ultra high-vacuum DC magnetron sputtering. (b) Step 2, formation of linear cracks by applying a tensile strain to the PDMS/PdNi sample. (c) Step 3, release of the applied tensile strain. (d) Step 4, formation of nanogaps in the PdNi thin film by utilizing the volumetric change of Pd—Ni upon exposure to H_2.
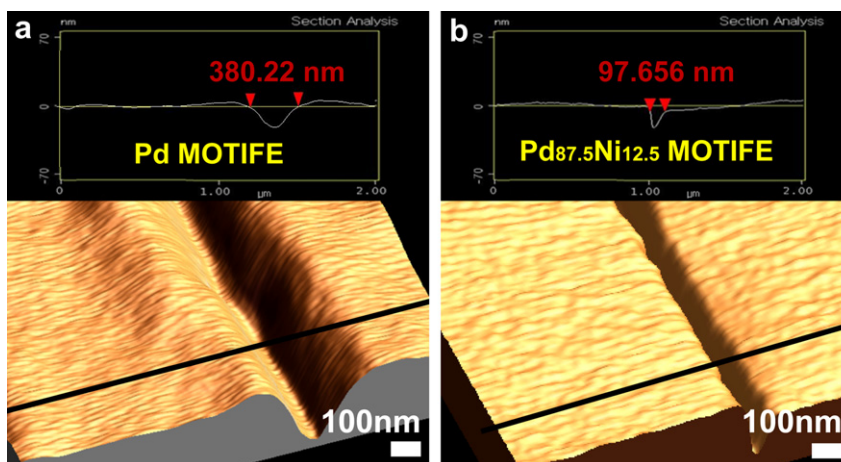
Fig. 2 – AFM images of a Pd film and a $Pd_{87.5}Ni_{12.5}$ film surface. The gaps under analysis are marked with red arrows: (a) A gap in a pure Pd MOTIFE has the gap width of 380 nm on top and an average width of 218 nm, and (b) A gap in a $Pd_{87.5}Ni_{12.5}$ MOTIFE exhibits the average width of 61.8 nm, about one-third of the presented Pd nanogap. (For interpretation of the references to colour in this figure legend, the reader is referred to the web version of this article.)

one-third of the Pd nanogap, as shown in Fig. 2(b). This demonstrates that adding a small amount of Ni to Pd can effectively reduce the gap width down to sub-100 nm. The reduced gap width in Pd–Ni film may be ascribed to the increase in ductility and fracture toughness [13], which has its origin in material characteristics of Ni that show higher ductility and toughness than those of Pd [14]. The Pd–Ni film with enhanced ductility and toughness can withstand the applied strain better and elongate more than pure Pd before it breaks, resulting in the narrower nanogap width. The nanogap-containing Pd–Ni films stay in the electrical Off state (open gap state) in the absence of H_2 because the gaps obstruct free current conduction. On exposure to H_2, the broken Pd–Ni films expand to be overlapped with neighboring films at the original gap positions, which turn the films to an electrical On state (closed gap state). In this mechanism, the nanogap width determines the smallest amount of H_2 that can be detected since the narrower gap can be closed with a less amount of volume expansion.

To measure the variations in electrical current during gas absorption and desorption, samples were first exposed to N_2 for stabilization, then to a desired concentration of H_2, and then back to N_2, thus completing one cycle. Fig. 3(a) shows the current change of a $Pd_{87.5}Ni_{12.5}$ MOTIFE measured by decreasing the H_2 concentration from 10 to 0.01%. The alloy MOTIFE operates in a perfect On-Off mode over the measured H_2 concentration range. Compared to the pure Pd MOTIFE, which detected only 0.4% of H_2 at minimum [11], this Pd–Ni alloy MOTIFE apparently exhibits a substantial reduction in the H_2 detection limit down to 0.01%, amounting a 97.5% decrease from that of the Pd MOTIFE. The significant reduction can be attributed first to the considerable decrease in the nanogap width as mentioned above and also to the increased expandability of Pd–Ni alloy films, which will be discussed later. The sensitivity, defined as resistance change relative to the initial resistance $(= |R\text{-}R_0|/R_0)$, reaches 100% at the extremely dilute hydrogen concentrations (0.05–0.01%), as shown in Fig. 3(b). Note that the sensitivity of the resistive type

sensor with the same film thickness was only 3.92% at 2% H_2 [11]. The average response times are less than 1 s for 0.05–0.02% H_2. As it recovers back to the OFF state upon disconnecting the H_2 flow, it is free from the base line fluctuation that has been pointed out as a common problem for conventional resistive type sensors.

Another important effect of alloying Pd with Ni can be found in current variations in response to high H_2 concentrations, as shown in Fig. 3(c). Unlike Pd MOTIFE sensors, which showed saturation in the variation above 2% of H_2,
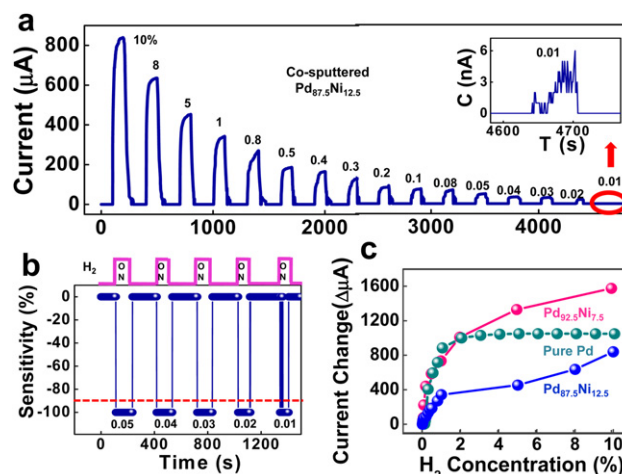

Fig. 3 – (a) The real-time electrical response of a $Pd_{87.5}Ni_{12.5}$ MOTIFE to H_2 in N_2 carrier at room temperature. The hydrogen concentrations are shown in percentages on top of the electrical response. (b) The sensitivity vs. time curve for the $Pd_{87.5}Ni_{12.5}$ MOTIFE. The sensitivity was converted from the electrical resistance response. The average response times are less than 1 s for 0.05–0.02% H_2 (The time interval between data points is 1 s). (c) The current variation vs. H_2 concentration curve for pure Pd and Pd–Ni based MOTIFEs ($Pd_{92.5}Ni_{7.5}$ and $Pd_{87.5}Ni_{12.5}$) in response to 0–10% H_2. For both types of MOTIFEs the film thickness was 10 nm.

Pd–Ni MOTIFEs ($Pd_{92.5}Ni_{7.5}$ and $Pd_{87.5}Ni_{12.5}$) exhibits different current variations commensurate with H_2 concentrations in the H_2 concentration range above 2%. For pure Pd films, a phase transition from the α to the β phase, in which the amount of incorporated H atoms exceeds the maximum H solid solubility, occurs around 2% H_2. As a result, the current change significantly increases beyond that point and then it is almost saturated at higher H_2 concentrations. The Ni inclusion in Pd suppresses the α to β phase transition [15,16], leading to the linear response behavior over a broad H_2 range. Although this scalable response to high H_2 concentrations is desirable, the overall sensitivity of the Pd–Ni films appears to be greatly decreased with increasing the Ni content (see Fig. 3(c) for a general trend). This is because more Ni inclusion in Pd raises the film resistance more [17] and makes hydrogen solubility and volume expandability of the film worse [18].

Ni inclusion also affects the relative volume change ($\Delta V/\Omega$), the ratio of volume expanded by hydrogen absorption (ΔV) to the initial metal volume (Ω). Fig. 4 displays the relative volume change as a function of Ni concentration. At room temperature, the relative volume changes of Pd and Ni are known to be 0.19 ± 0.01 and 0.28 [19], respectively. Provided that the volume change by an H atom incorporated is the same for Pd and Ni unit cells, the relative volume change depends on the unit cell volume. By XRD analysis, we calculated the lattice parameters and the relative volume changes of Pd–Ni films with different compositions [20]. The $Pd_{87.5}Ni_{12.5}$ XRD peak shifts by $0.40°$ to the right with respect to the Pd peak, corresponding to a 0.9% decrease in the lattice constant and accordingly a 2.6% increase in $\Delta V/\Omega$ from those of pure Pd. In this context, increasing the content of Ni brings about the corresponding increase in the relative volume change. The increased $\Delta V/\Omega$ value allows the alloy films to expand further when they absorb the same amount of hydrogen atoms, resulting in the consequent gap-closure even at low H_2 concentrations. Therefore the Ni addition to the Pd matrix can b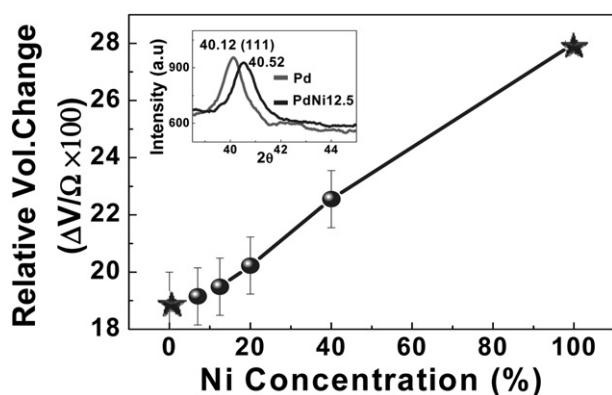e a powerful method for the extreme reduction of achieving a substantial reduction in the H_2 detection limit through this enhanced expandability in conjunction with the reduction of the nanogap width.

Nevertheless, 20% of Ni addition returned a detection limit of 0.02% as a result, which was rather higher than that of the $Pd_{87.5}Ni_{12.5}$ MOTIFE. This is due to the hydrogen solubility decrease at that alloy composition. The hydrogen solubility x ($=nH/(nPd + nNi)$) can be represented by Sieverts' law as $10^3x = ap^{1/2} + bp$, where p is the equilibrium pressure of hydrogen and a and b are Sieverts' constants. It is known that the values of a and b significantly decrease near 20% Ni [18], which causes a dramatic decrease in the solubility of H atoms at 15–20% of Ni contents [17]. The decreased H solubility at high Ni contents results in a volume expansion insufficient to close the gaps, leading to a decline in the reactivity with low concentrations of H_2 despite the increase in $\Delta V/\Omega$ and the decrease in nanogap width. Based on the observed results, the optimal Ni content was determined to be approximately 12.5% in Pd–Ni alloy MOTIFEs.

4.   Summary

We have effectively decreased the width of nanogaps below 100 nm by alloying Pd with Ni on the flexible PDMS substrate. The Pd–Ni MOTIFEs function as a highly sensitive hydrogen sponge in the respect that they close and open the nanogaps readily through the volumetric change of the Pd–Ni films during H_2 absorption and desorption. The sensors exhibited superior sensing properties such as extremely low detection limit, dynamic current change, short response time, enhanced concentration scalability, and broad hydrogen detection range. Particularly, the $Pd_{87.5}Ni_{12.5}$ MOTIFE showed fast On-Off switching with an ultra-low detection limit of 0.01% due to the reduced gap size and the increased relative volume change of the film. This novel method enables one to control the size of nanoscale gaps with ease and to create nanogaps over large areas in various metals on a flexible substrate. This method is also expected to be used for various fields such as nano-pattering, chemical sensors, and micro-fluidic channels as well.

Fig. 4 – Relative volume change ($\Delta V/\Omega \times 100$) vs. Ni concentration. Relative volume changes of pure Pd and Ni ($\star$) were cited from a reference [19] and those for Pd–Ni alloys ($Pd_{93}Ni_7$, $Pd_{87.5}Ni_{12.5}$, $Pd_{80}Ni_{20}$, and $Pd_{60}Ni_{40}$, $\bullet$) were calculated based on lattice parameter changes of the alloy films measured by XRD analysis. The inset shows the XRD peak of the $Pd_{87.5}Ni_{12.5}$ film shifts by $0.36°$ to the right compared to the Pd peak, resulting in a 2.6% increase in $\Delta V/\Omega$ from that of pure Pd.

Appendix A. Supplementary material

Supplementary material associated with this article can be found, in the online version, at http://dx.doi.org/10.1016/j.ijhydene.2012.07.004.

REFERENCES

[1] Strachan DR, Smith DE, Johnston DE, Park TH, Therien MJ, Bonnell DA, et al. Controlled fabrication of nanogaps in ambient environment for molecular electronics. Appl Phys Lett 2005;86:043109 (3pp).

[2] Wei D, Liu Y, Cao L, Wang Y, Zhang H, Yu G. Real time and in Situ control of the gap size of Nanoelectrodes for molecular devices. Nano Lett 2008;8:1625−30.

[3] Yi M, Jeong KH, Lee LP. Theoretical and experimental study towards a nanogap dielectric biosensor. Biosens Bioelectron 2005;20:1320−6.

[4] Favier F, Walter EC, Zach MP, Benter T, Penner RM. Hydrogen sensors and Switches from electrodeposited palladium mesowire arrays. Science 2001;293:2227−31.

[5] Kiefer T, Favier F, Vazquez-Mena O, Villanueva G, Brugger J. A single nanotrench in a palladium microwire for hydrogen detection (9pp). Nanotechnology 2008;19:125502.

[6] Yang F, Taggart D, Penner RM. Joule-heating a Palladium nanowire sensor for accelerated response and recovery to hydrogen gas. Small 2010;6:1422−9.

[7] Yang F, Kung S, Cheng M, Hemminger J, Penner RM. Smaller is Faster and more sensitive: the effect of Wire size on the detection of hydrogen by single palladium Nanowires. ACS Nano 2010;4:5233−44.

[8] Kim K, Cho SM. Pd nanowire sensors for hydrogen detection. Proc IEEE Sens 2004;2:705−7.

[9] Cherevko S, Kulyk N, Fu J, Chung CH. Hydrogen sensing performance of electrodeposited conoidal palladium nanowire and nanotube arrays. Sens Actuators B 2009;136:388−91.

[10] Ramanathan M, Skudlarek G, Wang HH, Darling SB. Crossover behavior in the hydrogen sensing mechanism for palladium ultrathin films (6pp). Nanotechnology 2010;21: 125501.

[11] Lee J, Shim W, Lee E, Noh JS, Lee W. Highly mobile palladium thin films on an elastomeric substrate: nanogap-based hydrogen gas sensors. Angew Chem Int Ed 2011;50:5301−5.

[12] Duffy DC, McDonald JC, Schueller OJA, Whitesides GM. Rapid Prototyping of Microfluidic Systems in Poly(dimethylsiloxane). Anal Chem 1998;70:4974−84.

[13] Kamran S, Chen K, Chen L. Ab initio examination of ductility features of fcc metals. Phys Rev B 2009;79:024106 (8pp).

[14] Schlesinger M, Paunovic M. Modern electroplating. Wiley; 2010. p. 355−358.

[15] Cheng YT, Li Y, Lisi D, Wang WM. Preparation and characterization of Pd/Ni films for hydrogen sensing. Sens Actuators B 1996;30:11−6.

[16] Lee E, Lee JM, Lee E, Noh J, Joe JH, Jung B, et al. Hydrogen gas sensing performance of Pd−Ni alloy thin films. Thin Solid Films 2010;519:880−4.

[17] Barton JC, Green JAS, Lewis FA. Changes of electrode potential and electrical resistance as a function of the hydrogen content of some Pd+Ni and Pd+Rh alloys. Trans Faraday Soc 1966;62:960−70.

[18] Shamsuddin M. Hydrogen interaction in palladium alloys. J Less-Commom Met 1989;154:285−94.

[19] Peis H. Lattice strains due to hydrogen in metals. Topics in applied Physics, hydrogen in metals I. Springer-Verlag; 1978. 53−74.

[20] Bidwell LR. Unit-cell dimensions of Ni-Pd alloys at 25 and 900°C. Acta Cryst 1964;17:1473−4.